

Power System Stability Enhancement Using Unified Power Flow Controllers

Ali T. Al-Awami*, Mohammed A. Abido*, Youssef L. Abdel-Magid**

* Electrical Engineering Department, King Fahd University of Petroleum & Minerals, Dhahran 31261, Saudi Arabia

** Electrical Engineering Program, The Petroleum Institute, Abu Dhabi, UAE

Abstract — The use of the supplementary controllers of a unified power flow controller (UPFC) to damp low frequency oscillations is investigated. The potential of the UPFC supplementary controllers to enhance the dynamic stability is evaluated by measuring the electromechanical controllability through singular value decomposition (SVD) analysis. Individual designs of the UPFC controllers using particle swarm optimization (PSO) technique are discussed. A nonlinear, time-domain objective function is considered. The effectiveness of the proposed controllers on damping low frequency oscillations is tested through eigenvalue analysis and non-linear time simulation. For comparison, power system stabilizer (PSS) performance is also included.

Index Terms — Power system stability, particle swarm optimization, simultaneous stabilization, PSS, UPFC.

I. INTRODUCTION

As power demand grows rapidly and expansion in transmission and generation is restricted, power systems are today much more loaded than before. This causes the power systems to be operated near their stability limits. In addition, interconnection between remotely located power systems gives rise to low frequency oscillations in the range of 0.1-3.0 Hz. If not well damped, these oscillations may keep growing in magnitude until loss of synchronism results.

Power system stabilizers (PSSs) have been used in the last few decades to serve the purpose of enhancing power system damping to low frequency oscillations. PSSs have proved to be efficient in performing their assigned tasks. However, they may adversely affect voltage profile and may not be able to suppress oscillations resulting from severe disturbances, especially those which may occur at the generator terminals.

A wide spectrum of PSS tuning approaches has been proposed. These approaches have included damping torque concepts [1], H_∞ [2], and variable structure [3], and the different optimization and artificial intelligence techniques [4]-[5].

FACTS devices have shown very promising results when used to improve power system steady-state

performance. Because of the extremely fast control action associated with FACTS-device operations, they have been very promising candidates for utilization in power system damping enhancement.

A unified power flow controller (UPFC) is the most promising device in the FACTS concept. It has the ability to adjust the three control parameters, i.e. the bus voltage, transmission line reactance, and phase angle between two buses, either simultaneously or independently. A UPFC performs this through the control of the in-phase voltage, quadrature voltage, and shunt compensation. Till now, not much research has been devoted to the analysis and control of UPFCs.

Several trials have been reported in the literature to model a UPFC for steady-state and transient studies. Based on Nabavi-Iravani model [6], Wang developed a linearized UPFC model [7] which has been incorporated into the Heffron-Phillips model.

A number of control schemes have been suggested to perform the oscillation-damping task. Huang et al. [8] attempted to design a conventional fixed-parameter lead-lag controller for a UPFC installed in the tie line of a two-area system to damp the interarea mode of oscillation. Mok et al. [9] considered the design of an adaptive fuzzy logic controller for the same purpose. Dash et al. [10] suggested the use of a radial basis function NN for a UPFC to enhance system damping performance. Robust control schemes, such as H_∞ and singular value analysis, have also been explored [11]-[12]. To avoid pole-zero cancellation associated with the H_∞ approach, the structured singular value analysis have been utilized in [13] to select the parameters of the UPFC controller to have the robust stability against model uncertainties.

In this paper, singular value decomposition (SVD) is used to select the control signal which is most suitable for damping the electromechanical (EM) mode oscillations. This is done as SVD analysis can be readily used to evaluate the EM mode controllability of the PSS and the different UPFC controllers. A SMIB system equipped with a PSS and a UPFC controller is used in this study. The problem of damping controllers design is formulated as an optimization problem to be solved using PSO. The aim of the optimization is to search for

the optimum controller parameter settings that minimize a nonlinear time-domain error-based objective function. Eigenvalue analysis and non-linear simulation are used to assess the effectiveness of the proposed controllers to damp low frequency oscillations under different disturbances.

II. PROBLEM STATEMENT

Fig. 1 shows a SMIB system equipped with a UPFC. The UPFC consists of an excitation transformer (ET), a boosting transformer (BT), two three-phase GTO based voltage source converters (VSCs), and a DC link capacitors. The four input control signals to the UPFC are m_E , m_B , δ_E , and δ_B , where

- m_E is the excitation amplitude modulation ratio,
- m_B is the boosting amplitude modulation ratio,
- δ_E is the excitation phase angle, and
- δ_B is the boosting phase angle.

A. Power System Model

By applying Park's transformation and neglecting the resistance and transients of the ET and BT transformers, the UPFC can be modeled as [6]-[7]:

$$\begin{bmatrix} v_{Etd} \\ v_{Etdq} \end{bmatrix} = \begin{bmatrix} 0 & -x_E \\ x_E & 0 \end{bmatrix} \begin{bmatrix} i_{Ed} \\ i_{Eq} \end{bmatrix} + \begin{bmatrix} \frac{m_E \cos \delta_E v_{dc}}{2} \\ \frac{m_E \sin \delta_E v_{dc}}{2} \end{bmatrix} \quad (1)$$

$$\begin{bmatrix} v_{Btd} \\ v_{Btdq} \end{bmatrix} = \begin{bmatrix} 0 & -x_B \\ x_B & 0 \end{bmatrix} \begin{bmatrix} i_{Bd} \\ i_{Bq} \end{bmatrix} + \begin{bmatrix} \frac{m_B \cos \delta_B v_{dc}}{2} \\ \frac{m_B \sin \delta_B v_{dc}}{2} \end{bmatrix} \quad (2)$$

$$\begin{aligned} \dot{v}_{dc} &= \frac{3m_E}{4C_{dc}} [\cos \delta_E \quad \sin \delta_E] \begin{bmatrix} i_{Ed} \\ i_{Eq} \end{bmatrix} + \\ &\frac{3m_B}{4C_{dc}} [\cos \delta_B \quad \sin \delta_B] \begin{bmatrix} i_{Bd} \\ i_{Bq} \end{bmatrix} \end{aligned} \quad (3)$$

where v_{Et} , i_E , v_{Bt} , and i_B are the excitation voltage, excitation current, boosting voltage, and boosting current, respectively; C_{dc} and v_{dc} are the DC link capacitance and voltage, respectively.

The non-linear model of the SMIB system of Fig. 1 is the 4th-order model used in [7].

The non-linear dynamic equations can be linearized around a given operating point to have the linear model given below:

$$\dot{x} = Ax + Bu \quad (8)$$

where

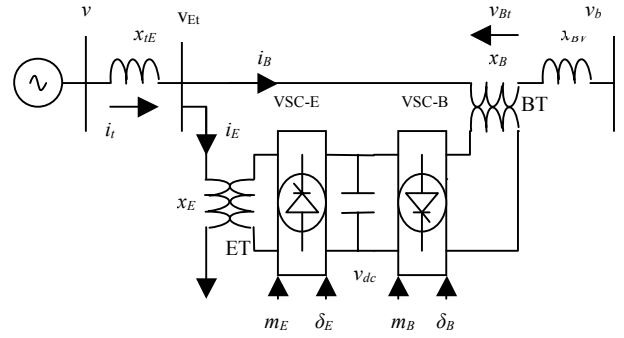


Fig. 1. SMIB power system equipped with UPFC

$$\begin{aligned} x &= [\Delta\delta \quad \Delta\omega \quad \Delta E'_q \quad \Delta E_{fd} \quad \Delta v_{dc}]^T \\ u &= [\Delta u_{pss} \quad \Delta m_E \quad \Delta \delta_E \quad \Delta m_b \quad \Delta \delta_b]^T \\ A &= \begin{bmatrix} 0 & \omega_b & 0 & 0 & 0 \\ -\frac{K_1}{M} & -\frac{D}{M} & -\frac{K_2}{M} & 0 & -\frac{K_{pd}}{M} \\ -\frac{K_4}{T'_{do}} & 0 & -\frac{K_3}{T'_{do}} & 1 & -\frac{K_{qd}}{T'_{do}} \\ -\frac{K_A K_5}{T_A} & 0 & -\frac{K_A K_6}{T_A} & -\frac{1}{T_A} & -\frac{K_A K_{vd}}{T_A} \\ \frac{K_7}{K_7} & 0 & \frac{K_8}{K_8} & 0 & -K_9 \end{bmatrix} \\ B &= \begin{bmatrix} 0 & 0 & 0 & 0 & 0 \\ 0 & -\frac{K_{pe}}{M} & -\frac{K_{p\delta e}}{M} & -\frac{K_{pb}}{M} & -\frac{K_{p\delta b}}{M} \\ 0 & -\frac{K_{qe}}{T'_{do}} & -\frac{K_{q\delta e}}{T'_{do}} & -\frac{K_{qb}}{T'_{do}} & -\frac{K_{q\delta b}}{T'_{do}} \\ \frac{K_A}{T_A} & -\frac{K_A K_{ve}}{T_A} & -\frac{K_A K_{v\delta e}}{T_A} & -\frac{K_A K_{vb}}{T_A} & -\frac{K_A K_{v\delta b}}{T_A} \\ 0 & K_{ce} & K_{c\delta e} & K_{cb} & K_{c\delta b} \end{bmatrix} \end{aligned}$$

M and D are the inertia constant and damping coefficient, respectively; ω_b the synchronous speed; δ and ω the rotor angle and speed, respectively; E'_q , E_{fd} , and v the generator internal, field and terminal voltages, respectively; T'_{do} the open circuit field time constant; x_d , x'_d and x_q the d-axis reactance, d-axis transient reactance, and q-axis reactance, respectively; K_A and T_A the exciter gain and time constant, respectively; V_{ref} the reference voltage; and u_{pss} the PSS control signal; P_m and P_e are the input and output power, respectively; $K_1 - K_9$, K_{pw} , K_{qw} and K_{vu} are linearization constants.

B. PSS and UPFC Controllers

The PSS structure to be considered is the very widely used lead-lag controller, whose transfer function is

$$u_{pss} = K \frac{sT_w}{1+sT_w} \left(\frac{1+sT_1}{1+sT_2} \right) \left(\frac{1+sT_3}{1+sT_4} \right) \Delta\omega \quad (9)$$

The UPFC damping controllers are of the structure shown in Fig. 2, where u can be m_E , δ_E , m_B , or δ_B . In order to maintain the power balance between the series and shunt converters, a DC voltage regulator must be incorporated. The DC voltage is controlled through modulating the phase angle of the ET voltage, δ_E . Therefore, the δ_E damping controller to be considered is that shown in Fig. 3, where the DC voltage regulator is a PI-controller.

C. Objective Function and Stabilizer Design

To select the best stabilizer parameters that enhance most the power system transient performance, the problem is formulated so as to optimize a selected objective function J subject to some inequality constraints. To avoid using an approximate linearized model, a nonlinear time-domain objective function is considered. It is worth noticing that the linearized model presented in Section 3 is used only for controllability assessment of the control signals. In the controller design stage, however, the nonlinear model is used directly.

In this work,

$$J = \int_0^{\infty} t |\Delta\omega| dt \quad (10)$$

Hence, the design problem can be formulated as:

minimize J
Subject to

$$K^{\min} \leq K \leq K^{\max}$$

$$T_1^{\min} \leq T_1 \leq T_1^{\max}$$

$$T_2^{\min} \leq T_2 \leq T_2^{\max}$$

$$T_3^{\min} \leq T_3 \leq T_3^{\max}$$

$$T_4^{\min} \leq T_4 \leq T_4^{\max}$$

where K and T_1 - T_4 are the controller gain and time constants, respectively.

The proposed approach employs PSO to search for the optimum parameter settings of the given controllers.

III. CONTROLLABILITY MEASURE

To measure the controllability of the EM mode by a given input (control signal), the singular value decomposition (SVD) is employed. The matrix B can be written as $B=[b_1 \ b_2 \ b_3 \ b_4 \ b_5]$ where b_i is a column vector corresponding to the i -th input. The minimum singular value, σ_{min} , of the matrix $[\lambda I - A \ b_i]$ indicates the capability of the i -th input to control the mode

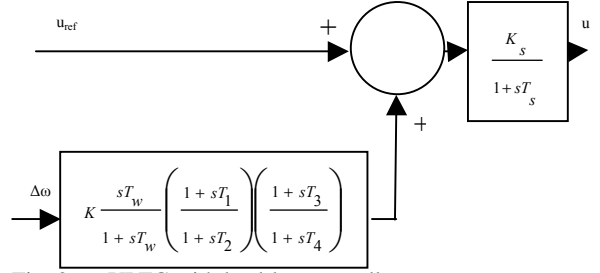


Fig. 2. UPFC with lead-lag controller

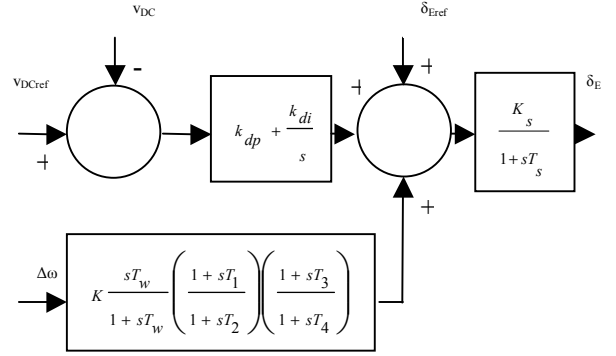


Fig. 3. UPFC with lead-lag controller and DC voltage regulator

associated with the eigenvalue λ . Actually, the higher the σ_{min} , the higher the controllability of this mode by the input considered. As such, the controllability of the EM mode can be examined with all inputs in order to identify the most effective one to control the mode. [14]-[15]

IV. PARTICLE SWARM OPTIMIZATION

Particle Swarm Optimization (PSO) was introduced first in [18]. This new approach features many advantages; it is simple, fast and can be coded in few lines. Also, its storage requirement is minimal.

Moreover, this approach is advantageous over evolutionary and genetic algorithms in many ways. First, PSO has memory. That is, every particle remembers its best solution (local best - $pbest$) as well as the group best solution (global best - $gbest$). Another advantage of PSO is that the initial population of the PSO is maintained, and so there is no need for applying operators to the population, a process that is time- and memory-storage-consuming. [16]-[17]

PSO starts with a population of random solutions "particles" in a D-dimension space. The i th particle is represented by $X_i=(x_{i1}, x_{i2}, \dots, x_{iD})$. PSO consists of, at each step, changing the velocity of each particle toward its $pbest$ and $gbest$ according to (20). The velocity of particle i is represented as $V_i=(v_{i1}, v_{i2}, \dots, v_{iD})$. The position of the i th particle is then updated according to (21) [16]-[17].

$$v_{id} = w*v_{id} + c_1*rand()* (p_{id}-x_{id}) + c_2*Rand()* (p_{gd}-x_{id}) \quad (20)$$

$$x_{id} = x_{id} + v_{id} \quad (21)$$

where, $p_{id} = p_{best}$ and $p_{gd} = g_{best}$

An excellent simplified description of the PSO algorithm can be referred to in [18]. A similar procedure to that presented in [18] has been employed here.

V. SIMULATION RESULTS

A. Controllability Measure

SVD is employed to measure the controllability of the EM mode from each of the five inputs: u_{pss} , m_E , δ_E , m_B , and δ_B . The minimum singular value, σ_{min} , is estimated over a wide range of operating conditions. For SVD analysis, P_e ranges from 0.05 to 1.4 pu and $Q_e = [0, 0.4]$. At each loading condition, the system model is linearized, the EM mode is identified, and the SVD-based controllability measure is implemented.

For comparison purposes, the minimum singular value for all inputs at $Q_e = 0.0$ and 0.4 pu is shown in Fig. 4 and Fig. 5, respectively.

From these figures, the following can be noticed:

- EM mode controllability via δ_E is always higher than that of any other input.
- The capabilities of δ_E and m_B to control the EM mode is higher than that of PSS.
- The EM mode is more controllable with PSS than with either m_E or δ_B .
- Generally, all control signals, except m_B at unity power factor and δ_E , suffer from low controllability to EM mode at light loading conditions.

B. Stabilizer Design

The PSO algorithm has been applied to search for the optimal parameter settings of each of the supplementary controllers so that the objective function is optimized. It is worth mentioning that the DC voltage regulator gains, k_{dp} and k_{di} , have been set a priori to the values shown in the Appendix. The final parameter settings of the supplementary controllers and the corresponding J are given in Table I. Notice that the optimization process has been carried out with the system operating at nominal loading condition given in Table II.

It is worth pointing out that the optimization of the m_E - and δ_B -based stabilizers parameter settings gives rise to poorly damped EM modes. Hence, these stabilizers and their results are excluded from the analysis hereafter.

The system EM modes and their corresponding damping ratios with the proposed PSS, m_B - and δ_E -based stabilizers when applied at the three loading conditions

shown in Table II (nominal, light, and heavy) are given in Table III. It is evident that, using the proposed stabilizers design, the damping ratio of the EM mode eigenvalue is greatly enhanced.

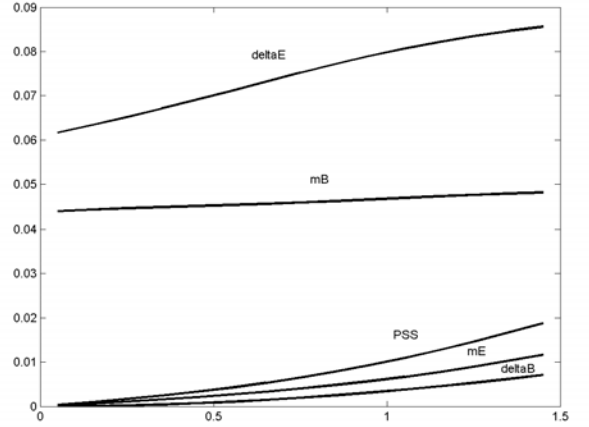


Fig. 4. Minimum singular value with all stabilizers at $Q_e=0.0$

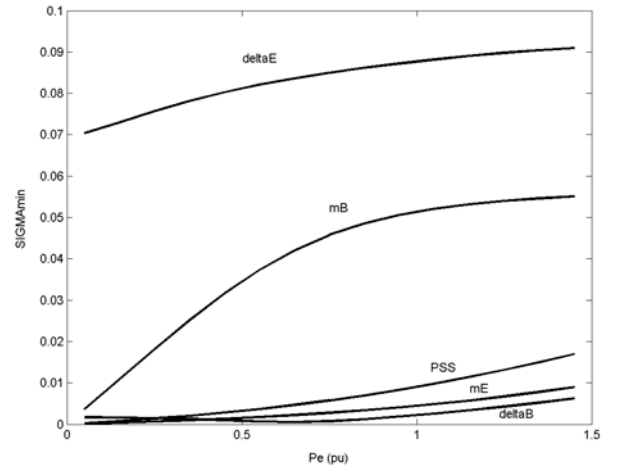


Fig. 5. Minimum singular value with all stabilizers at $Q_e=0.4$

TABLE I
THE OPTIMAL PARAMETER SETTINGS OF THE
INDIVIDUAL DESIGNS

	PSS	δ_E	m_B
K	100.00	100.00	100.00
T₁	0.08	5.00	0.15
T₂	0.01	1.17	0.01
T₃	3.53	0.05	5.00
T₄	5.00	1.11	3.57
J	12.64	14.50	25.20

TABLE II
SYSTEM OPERATING CONDITIONS

	P_e	Q_e
Nominal	1.000	0.015
Light	0.300	0.015
Heavy	1.100	0.400

C. Eigenvalue Analysis and Time-Domain Simulations

Moreover, the nonlinear time-domain simulations are carried out at the nominal and light loading conditions specified previously. The speed deviations for a 6-cycle three-phase fault at nominal and light loading are shown in Fig. 6 and Fig. 7, respectively.

From these results, it can be concluded that:

- m_B - and δ_E -based stabilizers provide the least overshoot during the first swing.
- The performance of δ_E -based stabilizer is almost unaffected with loading conditions. This ensures the robustness of this stabilizer.
- At light loading, δ_E -based stabilizer is the most effective in damping low frequency oscillations. The performance of PSS, however, is degraded at this loading condition.

In addition, the rotor angle response for a 6-cycle three-phase fault at light loading is shown in Fig. 8. This figure clearly shows that the δ_E -based stabilizer causes a substantial improvement in first swing stability over the other two stabilizers.

Generally, these results confirm those conclusions drawn from SVD analysis and eigenvalue analysis results.

VI. CONCLUSION

In this paper, SVD has been employed to evaluate the EM mode controllability to PSS and the four UPFC control signals. It has been shown that the EM mode is most strongly controlled via δ_E for a wide range of loading conditions. In addition, SVD analysis has illustrated that the EM mode is poorly controlled through m_E and δ_B .

An optimization technique has been proposed to design the PSS and UPFC controllers individually. PSO has been utilized to search for the optimal controller parameter settings that optimize a nonlinear time-domain objective function. Simulation results through nonlinear power system model have proved the conclusions drawn from linear SVD and eigenvalue analyses.

ACKNOWLEDGEMENT

The authors would like to acknowledge King Fahd University of Petroleum & Minerals for the support of this work under Project # KFUPM EE/Power/282.

APPENDIX

The test system parameters are:

Machine: $x_d=1$; $x_q=0.6$; $x'_d=0.3$; $D=0$; $M=8.0$; $T'_{do}=5.044$; $freq=60$; $v=1.05$;

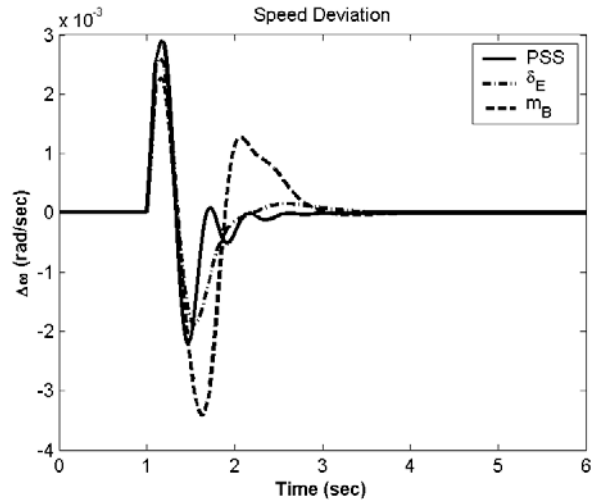


Fig. 6. Speed response to 6-cycle fault disturbance for nominal loading

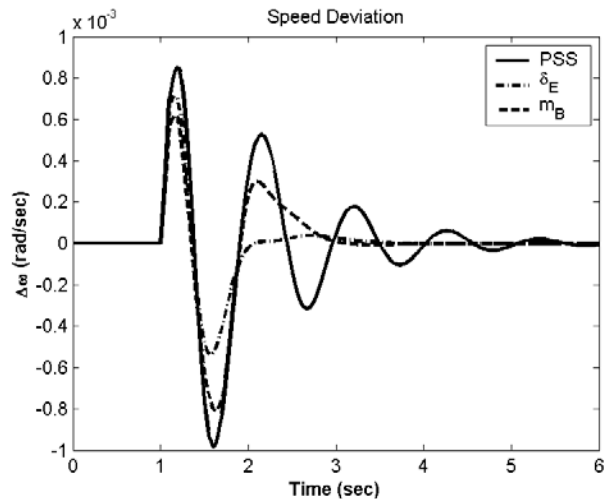


Fig. 7. Speed response to 3-cycle fault disturbance for light loading

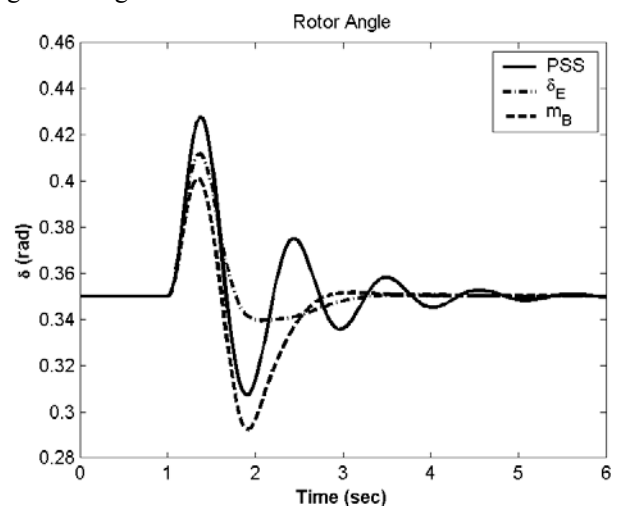


Fig. 8. Rotor angle response to 3-cycle fault disturbance for light loading

TABLE III

SYSTEM EIGENVALUES AND DAMPING RATIOS WITH AND WITHOUT CONTROL AT DIFFERENT LOADING CONDITIONS

Loading	No Control	PSS	δ_E	m_B
Nominal	$0.09 \pm 3.52i$, -0.02	$-3.63 \pm 13.86i$, 0.25	$-4.17 \pm 8.79i$, 0.43	$-4.58 \pm 12.23i$, 0.35
Light	$-0.44 \pm 3.35i$, 0.13	$-1.04 \pm 5.94i$, 0.17	$-3.76 \pm 7.98i$, 0.43	$-4.43 \pm 11.68i$, 0.35
Heavy	$0.14 \pm 3.39i$, -0.04	$-3.87 \pm 13.53i$, 0.27	$-3.84 \pm 9.67i$, 0.37	$-4.20 \pm 12.61i$, 0.32

Exciter : $K_A=50$; $T_A=0.05$; $E_{fd_max}=7.3$; $E_{fd_min}=-7.3$;
PSS: $T_w=5$; $T_{i_min}=0.05$; $T_{i_max}=1.5$; $i=1,2,3,4$; $upss_max=0.2$;
 $upss_min=-0.2$;
DC voltage regulator: $k_{dp}=-10$; $k_{di}=0$;
Transmission Line: $x_{LE}=0.1$; $x_{BI}=0.6$;
UPFC: $x_E=0.1$; $x_B=0.1$; $K_s=1$; $T_s=0.05$; $C_{dc}=3$; $V_{dc}=2$;
 $m_{E_max}=2$; $m_{E_min}=0$; $m_{B_max}=2$; $m_{B_min}=0$.

REFERENCES

- [1] M. J. Gibbard, "Co-ordinated design of multimachine power system stabilisers based on damping torque concepts," *IEE Proc. Pt. C*, Vol. 135, No. 4, 1988, pp. 276-284.
- [2] M. Klein, L.X. Le, G.J. Rogers, S. Farrokhpay, and N.J. Balu, "H ∞ damping controller design in large power systems," *IEEE Trans. Power Systems*, Vol. 10, no. 1, Feb. 1995, pp. 158-166
- [3] V. G. D. C. Samarasinghe and N. C. Pahalawatththa, "Damping of multimodal oscillations in power systems using variable structure control techniques," *IEE Proc. Gen. Trans. and Distrib.*, Vol. 144, No. 3, 1997, pp. 323-331.
- [4] Y.L. Abdel-Magid, M.A. Abido, S. Al-Baiyat and A. H. Mantawy, "Simultaneous Stabilization of Multimachine Power Systems via Genetic Algorithms," *IEEE Trans. Power Sys.*, Vol. 14, No. 4, November 1999, pp. 1428-1439.
- [5] M.A. Abido and Y.L. Abdel-Magid, "Radial basis function network based power system stabilizers for multimachine power systems," *Intl. Conf. Neural Networks*, Vol. 2, 9-12 June 1997, pp. 622-626
- [6] A. Nabavi-Niaki, M.R. Iravani, "Steady-state and dynamic models of unified power flow controller (UPFC) for power system studies," *IEEE Trans. Power Systems*, Vol. 11, No. 4, Nov. 1996, pp 1937-1943
- [7] H.F. Wang, "Damping function of unified power flow controller," *IEE Proc. Gen. Trans. and Distrib.*, Vol. 146, No. 1, 1999, pp 81-87.
- [8] Z. Huang, Y. Ni, C.M. Shen, F.F. Wu, S. Chen, B. Zhang, "Application of unified power flow controller in interconnected power systems-modeling, interface, control strategy, and case study," *IEEE Trans. Power Systems*, Vol. 15, No. 2, May 2000, pp 817-824
- [9] T.K. Mok, Y. Ni, F.F. Wu, "Design of fuzzy damping controller of UPFC through genetic algorithm," *IEEE Power Engineering Society Summer Meeting*, Vol 3, 16-20 July 2000, pp 1889 - 1894
- [10] P.K. Dash, S. Mishra, G. Panda, "A radial basis function neural network controller for UPFC," *IEEE Trans. Power Systems*, Vol. 15, No. 4, Nov. 2000, pp 1293-1299
- [11] M. Vilathgamuwa, X. Zhu, S.S. Choi, "A robust control method to improve the performance of a unified power flow controller," *Electric Power System Research*, 55, 2000, pp 103-111.
- [12] B.C. Pal, "Robust damping of interarea oscillations with unified power flow controller," *IEE Proc. Gen. Trans. and Distrib.*, Vol. 149, No. 6, 2002, pp 733-738.
- [13] J.C. Seo, S. Moon, J.K. Park, J.W. Choe, "Design of a robust UPFC controller for enhancing the small signal stability in the multi-machine power systems," *IEEE Power Engineering Society Winter Meeting*, 2001. Vol. 3, 28 Jan.-1 Feb. 2001, pp 1197-1202
- [14] A. M. A. Hamdan, "An investigation of the significance of singular value decomposition in power system dynamics," *Int. Journal of Electrical Power and Energy Systems*, 21, 1999, pp 417-424
- [15] Y.L. Abdel-Magid, M.A. Abido, "Robust coordinated design of excitation and TCSC-based stabilizers using genetic algorithm," *Electric Power System Research*, 69, 2004, pp 129-141.
- [16] J. Kennedy, R. Eberhart, "Particle swarm optimization," *Proc. IEEE Intl. Conf. Neural Networks*, 4, Nov/Dec 1995, pp 1942-1948.
- [17] R. Eberhart, J. Kennedy, "A new optimizer using particle swarm theory," *Proc. Sixth Intl. Symposium Micro Machine and Human Science*, 1995. MHS '95, 4-6 Oct 1995, pp 39-4
- [18] M. A. Abido, "Particle swarm optimization for multimachine power system stabilizer design," *IEEE PES Summer Meeting*, Vol. 3, 15-19 July 2001, pp. 1346-1351